Reactive power control of grid-connected wind farm based on adaptive dynamic programming

Yufei Tang [a], Haibo He [a,*], Zhen Ni [a], Jinyu Wen [b], Xianchao Sui [b]

[a] Department of Electrical, Computer, and Biomedical Engineering, University of Rhode Island, Kingston, RI 02881, USA
[b] College of Electrical and Electronic Engineering, Huazhong University of Science and Technology, Wuhan 430074, China

ARTICLE INFO

ABSTRACT

Optimal control of large-scale wind farm has become a critical issue for the development of renewable energy systems and their integration into the power grid to provide reliable, secure, and efficient electricity. Among many enabling technologies, the latest research results from both the power and energy community and computational intelligence (CI) community have demonstrated that CI research could provide key technical innovations into this challenging problem. In this paper, a neural network based controller is presented for the reactive power control of wind farm with doubly fed induction generators (DFIG). Specifically, we investigate the on-line learning and control approach based on adaptive dynamic programming (ADP) for wind farm control and integration with the grid. This controller can effectively dampen the oscillation of the wind farm system after the ground fault of the grid. Compared to previous control strategies, this controller is on-line and "model free", and therefore, can reduce the control complexity. Simulation studies are carried out in Matlab/Simulink and the results demonstrated the effectiveness of the ADP controller.

1. Introduction

The development of renewable energy for sustainable, efficient, and clean electric power systems has become a critical research topic world wide [1–4]. Among various renewable energy sources, wind power is the most rapidly growing one in the world. While the wind is random and intermittent, the major hurdle in developing such energy has been the lack of efficient control. In this paper, we focus on the adaptive dynamic programming (ADP) based reactive power control of the wind farm under grid fault.

In general, there are mainly three kinds of wind power generators: squirrel-cage induction generator, permanent magnet synchronous generator and doubly fed induction generator (DFIG). DFIG is widely used in the wind power system for its advantages over other two types [5]. The characteristics of DFIG are high efficiency, flexible control and low investment. The stator of DFIG is directly connected to the power grid while the rotor is connected to the power grid through a back-to-back converter, which only takes about 20–30% of the DFIG rated capacity for the reason that the converter only supplies the exciting current of the DFIG. The back-to-back converter consists of three parts: rotor side converter (RSC), grid side converter (GSC)

and DC Link capacitor. From the previous research, the controller of the converter has significant effect on the stability of grid-connected DFIG [6,7].

In the previous research, the stability analysis and optimal control of wind farm with DFIG have been studied in the community [8–16]. The key challenge for wind farm optimization is to build an accurate wind farm model and the involvement of a large number of parameters need to be optimized to ensure a good interaction of the wind farm with the power grid at the common coupling point (CCP). For instance, in [8], the authors proposed to use particle swarm optimization (PSO) to optimize the control parameters in a DFIG simultaneously. This method can improve the performance of the DFIG in the power grid, however, when the number of the DFIG in a wind farm increases, the number of the control parameters will increase significantly (i.e., curse of dimensionality issue). Fuzzy logic control has been successfully applied to control DFIG in different aspects. In [11], fuzzy logic control was implemented on primary frequency and active power control of the wind farm. In [12], Neuro-Fuzzy vector control was used and realized on a laboratory DFIG. Other advanced coordinated control approaches such as ADP based methods have shown promising results for such a challenging problem [17–20].

In [19], the authors proposed a heuristic dynamic programming (HDP) based coordinated reactive power control of a large wind farm and a STATCOM. This HDP controller can improve the

* Corresponding author.
  E-mail addresses: ytang@ele.uri.edu (Y. Tang), he@ele.uri.edu (H. He), ni@ele.uri.edu (Z. Ni), jinyu.wen@hust.edu.cn (J. Wen), 350405880@qq.com (X. Sui).

performance of the DFIG in the power grid when there is a grid fault. However, this HDP controller needs to be sufficiently pre-trained based on the information from the power system before connected to the grid. Motivated by our previous research on ADP [29,30,21], in this paper, we use the on-line ADP architecture as proposed in [22] for wind farm reactive power control. This ADP control method is "model free," that is to say without the requirement of a detail physical model as well as a complex model network to predict the system status [22]. This enables the ADP approach to learn "on-the-fly" while interacting with the power grid. This approach has been successfully demonstrated with many applications including stabilization and tracking control of an Apache helicopter [23,24], damping oscillation control in a classic "four machine two area" system, a large power system in China [25], among others [26–28]. In this paper, we aim to investigate the reactive power control of a wind farm connected to the power grid under fault condition.

The rest of the paper is organized as follows. Section 2 briefly introduces the DFIG wind system, RSC and GSC controller model. Detailed ADP control approach has been presented in Section 3. The power system scenario that we study in this work and simulation results are presented in Section 4. Finally, a conclusion is given in Section 5.

2. DFIG wind turbine system model

The wind turbine model studied in this paper is illustrated in Fig. 1. In this system, the wind turbine is connected to the DFIG through a drive train system, which consists of a low and a high speed shaft with a gearbox in between. The wind turbine (WT) with DFIG system is an induction type generator in which the stator windings are directly connected to the three-phase grid and the rotor windings are fed through three-phase back-to-back insulated-gate bipolar transistor (IGBT) based pulse width modulation (PWM) converters. The back-to-back PWM converter includes three parts: a rotor side converter (RSC), a grid side converter (GSC) and a DC Link capacitor placed between the two converters. Their controller also includes three parts: rotor side converter controller, grid side converter controller and wind turbine controller. The function of these controllers are to produce smooth electrical power with constant voltage and frequency to the power grid whenever the wind system is working at sub-synchronous speed or super-synchronous speed, depending on the velocity of the wind. Vector control strategy is employed for both the RSC controller and the GSC controller to achieve decoupled control of active and reactive power.

2.1. Model of drive train

The drive train system [8] includes the turbine, a low and a high speed shaft, and a gearbox. This system can be represented by a two-mass model as follows:

$$2H_t \frac{d\omega}{dt} = T_m - T_{sh} \tag{1}$$

$$\frac{d\theta_{tw}}{dt} = \omega_t - \omega_r = \omega_t - (1 - s_r)\omega_s \tag{2}$$

$$2H_g \frac{ds_r}{dt} = -T_{em} - T_{sh} \tag{3}$$

$$T_{sh} = K_{sh}\theta_{tw} + D_{sh}\frac{d\theta_{tw}}{dt} \tag{4}$$

where

H_t	the inertia constants of the turbine
H_g	the inertia constants of the generator
ω_t	the WT angle speed
ω_r	the generator rotor angle speed
$\theta_{t\omega}$	the shaft twist angle
K_{sh}	the shaft stiffness coefficient
D_{sh}	the damping coefficient
T_{sh}	the shaft torque
T_m	the wind torque
T_{em}	the electromagnetic torque

The maximum power coefficient may be achieved by controlling the WT speed in order to track the maximum power from wind. The tracking strategy for the DFIG is achieved by driving the generator speed along the optimum power speed characteristic curve, which corresponds to the maximum energy capture from the wind.

2.2. Model of DC Link capacitor

From Fig. 1, the active power flow through the back-to-back PWM converter is balanced by the DC Link capacitor [8]. The power balance equation can be represented as follows:
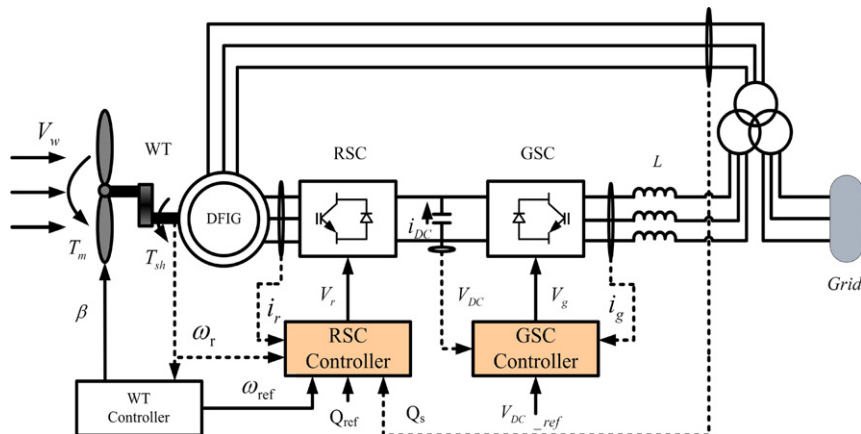
$$P_r = P_g + P_{DC} \tag{5}$$

Fig. 1. Schematic diagram of DFIG wind turbine system [13,14].

where

P_r	the active power at the AC terminal of the RSC
P_g	the active power at the AC terminal of the GSC
P_{DC}	the active power of the DC Link capacitor

2.3. Model of rotor side controller

As we mentioned before, the vector control strategy is used for the active power and reactive power control of the WT with DFIG system. For the RSC, the active power and voltage are controlled independently via v_{qr} and v_{dr}, respectively. The voltage control is achieved by controlling the reactive power to keep it within the desired range. Fig. 2 demonstrates the overall vector control scheme of the RSC. The rotor speeds w_r and Q_s are the measured system active power and reactive power, respectively. They are compared with the desired active power and reactive power to generate the reference signals i_{qr_ref} and i_{dr_ref}, respectively. The actual $d-q$ current signals i_{qr} and i_{dr} are then compared with these reference signals to generate the error signals, which are passed through two PI controllers to form the voltage signal reference v$_{qr}^*$ and v$_{dr}^*$, respectively. The two voltage signals v$_{qr}^*$ and v$_{dr}^*$ are compensated by the corresponding cross-coupling terms to form the voltage signals v_{qr} and v_{dr}, respectively. These signals are then sent to the PWM module to generate the IGBT gate control signal V_r to drive the rotor side converter.
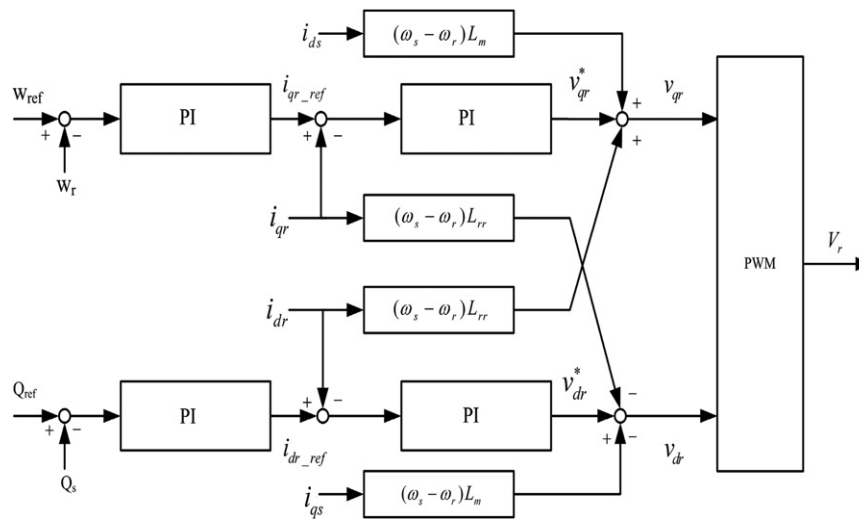
2.4. Model of grid side controller

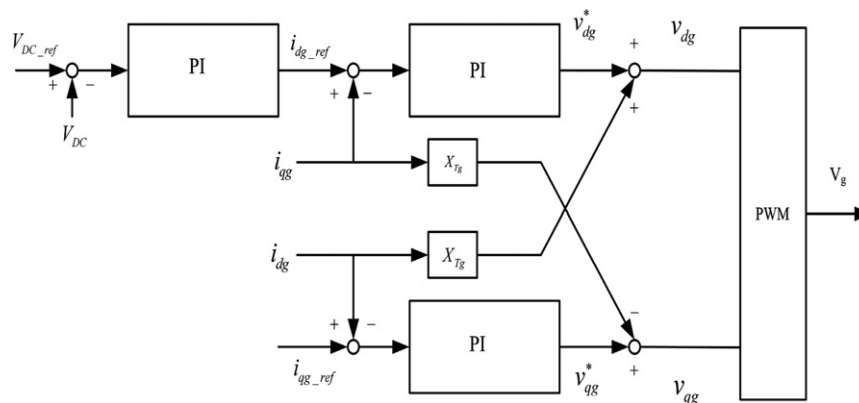The GSC, as shown in Fig. 3, aims to maintain the DC Link voltage and control the terminal reactive power. The DC Link voltage and reactive power are controlled independently via v_{dg} and v_{qg}, respectively. The actual signal of the DC Link voltage V_{DC} is compared with its command value V_{DC_ref} to form the error signal, which is passed through the PI controller to generate the reference signal i_{dg_ref}. Then this reference signal i_{dg_ref} and another corresponding reference signal i_{qg_ref} are compared with the actual values i_{qg} and i_{dg}, respectively. These error signals are then passed through two PI controllers to form the voltage signal reference v$_{dg}^*$ and v$_{qg}^*$, respectively. The two voltage signals v$_{dg}^*$ and v$_{qg}^*$ are compensated by the corresponding cross-coupling terms to form the voltage signals v_{dg} and v_{qg}, respectively. These are then send to the PWM module to generate the IGBT gate control signals V_g to drive the grid side converter.

3. DFIG wind turbine system with ADP controller

3.1. On-line model-free ADP

Fig. 4 is a basic control framework of on-line model-free ADP [22], where u is the control signal, and X is the state vector. The reinforcement signal r is obtained from the external environment which in this paper is the wind farm power system.
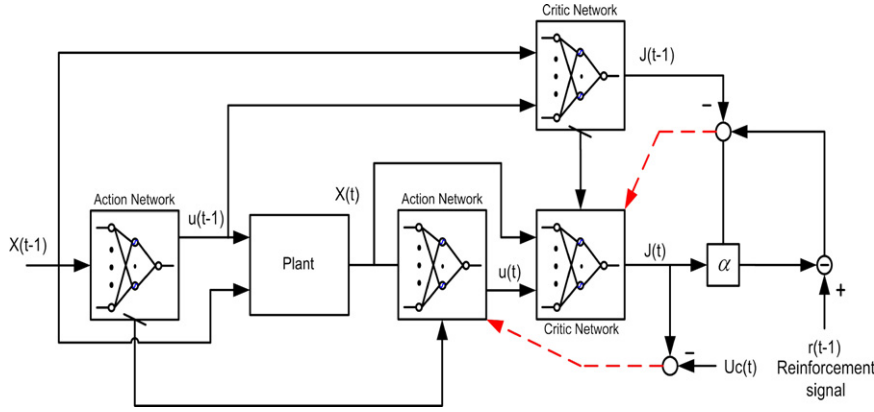

Fig. 2. Schematic diagram of rotor side controller.

Fig. 3. Schematic diagram of grid side controller.

Fig. 4. Schematic diagram of ADP [22].

ADP control comprises two main parts: an action network and a critic network. The action network produces control signal u according to a learning policy represented by the approximating network, while the critic network approximates the cost/reward function J of the Bellman equation in dynamic programming. These two parts are usually implemented by neural networks because of their universal approximation capabilities and the associated back-propagation learning algorithm.

During the initial on-line learning, the controller is "naive" when it starts to control, which means the action network and critic network are both randomly initialized in their weights. Once the system state vectors are observed, the control action will be subsequently produced based on the parameters in the action network.

The output of the critic network, the J function, approximates the discounted total reward-to-go. Specifically, it approximates $R(t)$ as follows:

$$R(t) = \sum_{k=1}^{\infty} \alpha^{k-1} r(t+k) \tag{6}$$

where $R(t)$ is the future accumulative reward-to-go value at time t and α is a discount factor for the infinite horizon problem ($0 < \alpha < 1$). The α equals to 0.95 in this paper.

The critic network is trained to approximate the function $J(t)$ by minimizing the objective function, which is given as follows:

$$e_c(t) = \alpha J(t) - [J(t-1) - r(t)] \tag{7}$$

$$E_C(t) = \tfrac{1}{2} e_c^2(t) \tag{8}$$

The weight update rule for the critic network is a gradient-based adaptation given by

$$w_c(t+1) = w_c(t) + \Delta w_c(t) \tag{9}$$

$$\Delta w_c(t) = l_c(t) \left[-\frac{\partial E_c(t)}{\partial w_c(t)} \right] \tag{10}$$

where $l_c(t) > 0$ is the learning rate of the critic network at time t, and w_c is the weight vector in the critic network.

The action network is trained to indirectly back propagate the error between the desired ultimate objective U_c and the approximate J function from the critic network. The weights in the action network are tuned by minimizing the following error function:

$$e_a(t) = J(t) - U_c(t) \tag{11}$$

$$E_a(t) = \tfrac{1}{2} e_a^2(t) \tag{12}$$

Therefore, the weights updated in the action network can be calculated as follows:

$$w_a(t+1) = w_a(t) + \Delta w_a(t) \tag{13}$$

$$\Delta w_a(t) = l_a(t) \left[-\frac{\partial E_a(t)}{\partial w_a(t)} \right] \tag{14}$$

where $l_a(t) > 0$ is the learning rate of the critic network at time t, and w_a is the weight vector in the critic network.

3.2. ADP based wind farm controller design

Fig. 5 demonstrates the proposed DFIG wind turbine system with ADP controller. The dashed line block denotes the wind farm to be controlled by the ADP controller. The voltage V at bus B_{575} and the active power P of the wind farm are fed into the ADP controller to produce the supplementary control signal ΔQ_{ref}, then add this signal with steady state command Q_{s0} to form the control signal Q_{ref} to the RSC controller of the DFIG. The lower part of this figure is the on-line ADP controller as discussed in [22]. The basic principle is that through control the reference signal Q_{ref}, the DFIG could generate or absorb reactive power to keep the voltage of DFIG at its desire set point. When the system is stable, the control signal Q_{ref} will be constant which means the reactive power will be constant as well. While the system is under disturbance or grid fault, the control signal Q_{ref} will be adaptively adjusted, which allows the DFIG to generate or absorb reactive power according to the situation. This change could reduce the level of voltage sags of the wind farm and at the CCP point. The control signal will also help to dampen the oscillation of the system after the disturbance is removed or grid fault is recovered. Because of the direct coupling between the voltage and the reactive power, it is straightforward to use the voltage V as an input signal of the ADP controller. The active power of the wind farm P will also be chosen as another input signal to provide additional information which will help the ADP controller to achieve better control performance [19].

3.3. Design of the critic network

Figs. 6 and 7 demonstrate the design of the critic network. It is a three-layer neural network with 6 hidden neurons. The inputs to the critic network are the measured system state vector $V(t)$, $P(t)$ and their one time-delayed values $V(t-1)$, $P(t-1)$, and the action network output ΔQ_{ref}. $r(t)$ is used to define the error function of the critic network, and not directly used as one of the input states to the critic network. The output of the critic network is the approximate discounted total toward-to-go function J.

As we have mentioned earlier, the objective of the ADP controller is to provide an optimal control signal that can reduce the level of voltage sags of the wind farm and at the CCP point, and also to dampen the oscillation of the system after the
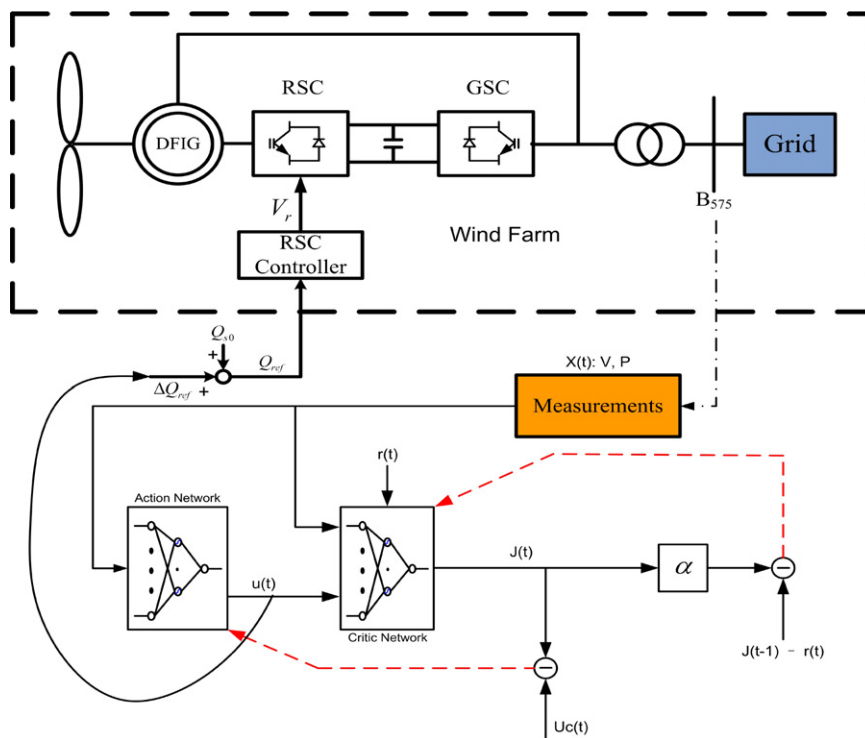
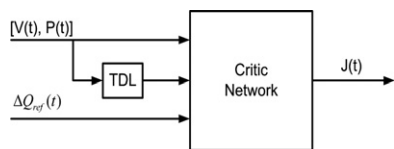**Fig. 5.** Schematic diagram of DFIG wind turbine system with ADP.
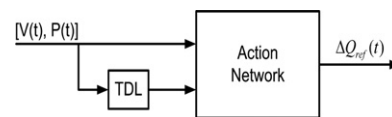

Fig. 6. Structure of critic network.

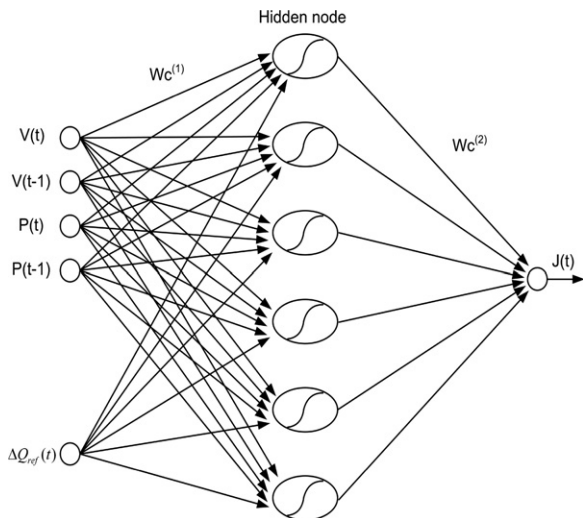**Fig. 8.** Structure of action network.

Fig. 7. Critic neural network with 5 inputs, 6 hidden layer neurons, and one output neuron.

disturbance is removed or grid fault is recovered. Therefore, we design the reinforcement signal $r(t)$ as follows:

$$r(t) = \tfrac{1}{2}[(V(t)-1.02)^2 + 0.6(V(t-1)-1.02)^2]$$

$$+ \tfrac{1}{2}[(P(t)-0.4)^2 + 0.6(P(t-1)-0.4)^2] \tag{15}$$

where the numbers 1.02 and 0.4 are the approximate per unit of voltage and active power of the wind farm in steady-state, respectively.

3.4. Design of the action network

Figs. 8 and 9 demonstrate the design of the action network, which is also a three-layer neural network with 6 hidden neurons similar to the critic network. The inputs to the action network are the measured system state vector $V(t)$, $P(t)$ and their one time-delayed values $V(t-1)$, $P(t-1)$. The output of the action network is the supplementary control signal ΔQ_{ref}.

4. Simulation results and analysis

4.1. Case 1: single machine infinite bus (SMIB) power system

We first introduce the SMIB power system application scenario in this section. Normally, there are tens to hundreds wind turbines in a large wind farm. Many existing research results have demonstrated that if the controller of the wind turbines is well-tuned, there will be no mutual interaction between wind turbines on a wind farm (i.e., these wind turbines are mutually independent [7]). In this paper, we take the same assumption meaning that we consider to represent the wind farm by one large WT with DFIG system. Fig. 10 shows the diagram of the simulated single wind farm infinite bus system. A 30 MW wind farm consisting of twenty 1.5 MW wind turbines connected to a
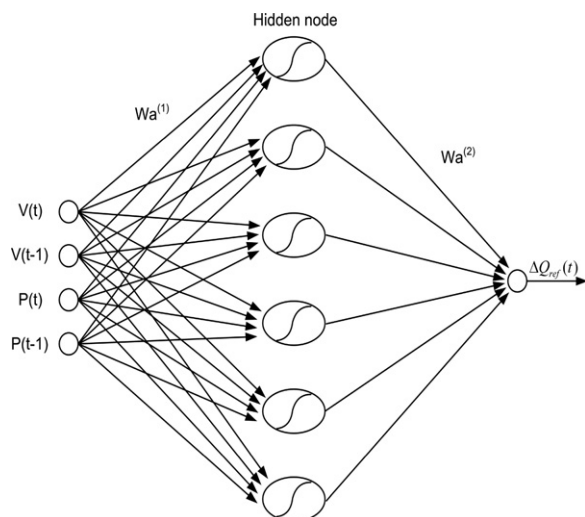
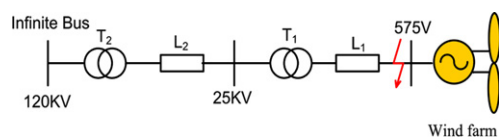**Fig. 9.** Action neural network with 4 inputs, 6 hidden layer neurons, and one output neuron.

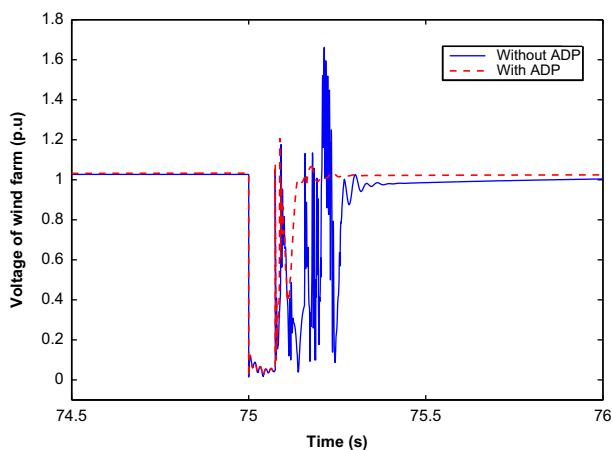**Fig. 10.** Single-line diagram of the benchmark power system includes a wind farm.

Fig. 11. Comparison of the wind farm voltage with and without ADP controller at B575.

25 kV distribution system exports power to a 120 kV grid through a 30 km, 25 kV feeder. This 120 kV grid represents an infinite bus to the wind farm. Wind turbines use DFIG consisting of a wound rotor induction generator and an AC/DC/AC insulated-gate bipolar transistor based pulse width modulation converters. The stator winding is connected directly to the 60 Hz grid while the rotor is fed at a variable frequency through the AC/DC/AC converter.

In the previous section, we have designed the ADP controller and demonstrated how to integrate it with the DFIG wind turbine system. We have implemented the whole system in Matlab/Simulink environment to verify the dynamic stability control by the ADP approach in this SMIB power system. Three-phase ground fault is applied in the simulation and the fault time is 75 ms. Because this paper focuses on the short-term stability of the WT system under disturbance, we assume that the wind
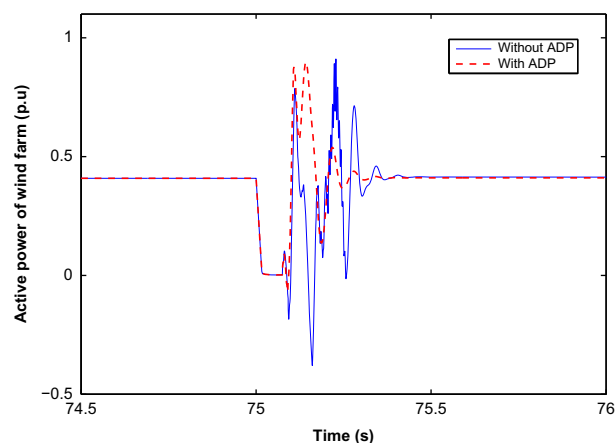

Fig. 12. Comparison of the wind farm active power with and without ADP controller.
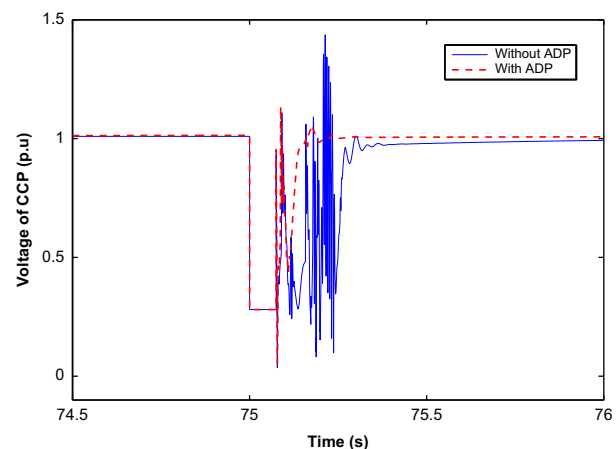

Fig. 13. Comparison of the CCP voltage with and without ADP controller at B25.

speed is constant at 10 m/s during the simulation. The dynamic performance of the wind farm with the ADP controller is compared with the case without the ADP controller.

Figs. 11, 12, and 13 are the simulation results for the wind farm voltage (575 V), wind farm active power, and CCP (25 KV) voltage, respectively. From these figures we can see that using the ADP controller, the dynamic performance of the wind farm has been significantly improved. The sag and overshot magnitudes of the active power P, voltage of the wind farm V_{575} and the voltage at the CCP V_{25} have been significantly reduced with the ADP controller. The oscillation damping performance with the ADP controller has also been improved with respect to the situation without the ADP controller.

4.2. Case 2: multi-machine power system

To verify the robustness of the proposed ADP controller, a multi-machine power system is also used in this paper. Fig. 14 demonstrates the revised four-machine-two-area system based on the classic model. This power system model was presented in [9] to investigate the impact of the wind turbine with different controllers such as the optimized PI controller and nonlinear controller. The system is divided into two areas, each with two machines. In [9], the four-machine-two-area system was modified by replacing generator G3 with a wind farm. In this paper, instead of replacing G3 with a wind farm, we replace G4 with a
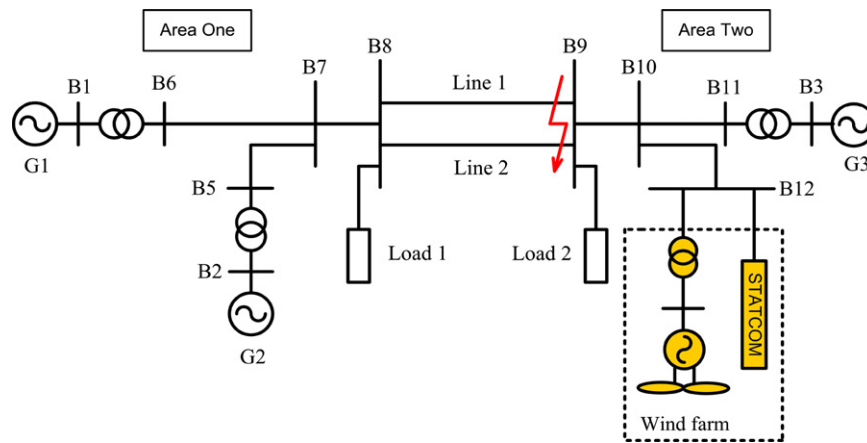
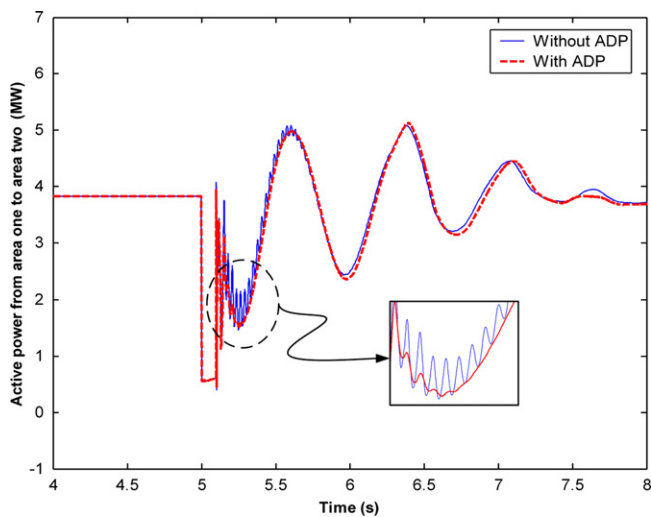**Fig. 14.** Single-line diagram of the benchmark power system that includes a wind farm and a STATCOM.

Fig. 15. Comparison of the active power from area one to area two with and without ADP controller.
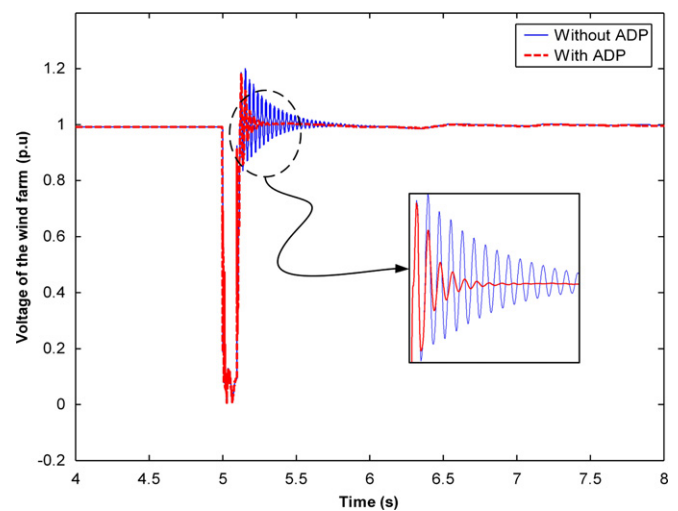

Fig. 16. Comparison of the wind farm voltage with and without ADP controller at B575.

wind farm and a static synchronous compensator (STATCOM). The penetration of the wind power is almost 25% of the whole system. The parameters of the system and the power flow can be found in [9].

Because the control object changes to one DFIG and one STATCOM, there will be two output signals of the ADP controller: ΔQ_{ref} for the DFIG and ΔV_{ref} for the STATCOM. The STATCOM is modeled as an IGBT based STATCOM, however, as details of the inverter and harmonics are not represented, it can be also used to model a gate-turn-off (GTO) thyristor based STATCOM in transient stability studies.

Figs. 15–20 demonstrate the simulation results of various variables of this benchmark under the situation of with and without the ADP controller. Specifically, Fig. 15 shows the active power transfer from area one to area two, Fig. 16 shows the wind farm voltage at B575, Fig. 17 shows the wind farm active power, Fig. 18 shows the rotor current of the DFIG, Fig. 19 shows the CCP voltage at B12, and Fig. 20 shows the reactive power of the STATCOM. From all these results, it can be observed that by applying the ADP controller, the system can improve its stability and damping characteristic after the fault. The oscillation of the system and the wind farm decayed very quickly after the fault was cleared. Fig. 20 also demonstrated that with the ADP controller, the reactive power output of the STATCOM meets the needs of the system under fault conditions. This suggests that
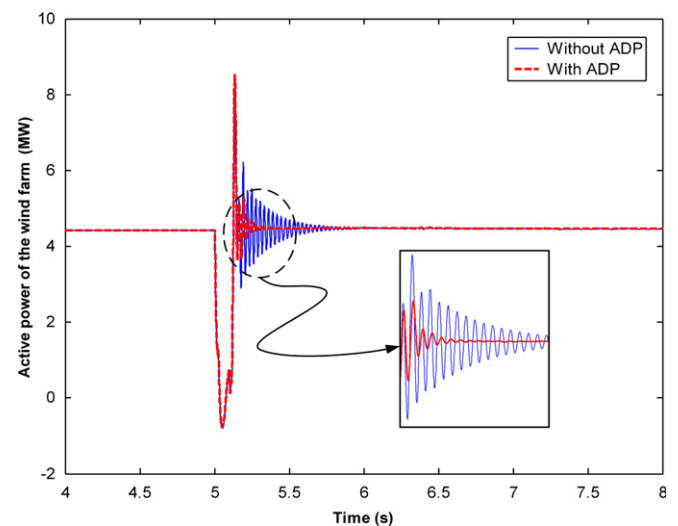

Fig. 17. Comparison of the wind farm active power with and without ADP controller.

during and after the fault, the STATCOM can provide sufficient reactive power to support the system voltage and dampen the oscillation.
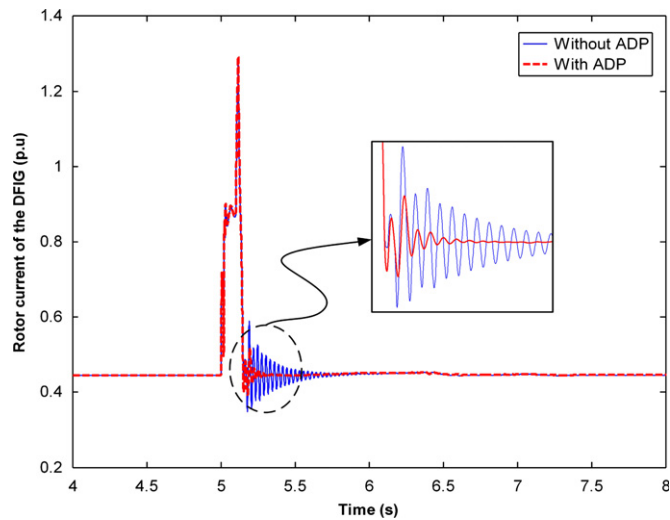
Fig. 18. Comparison of the rotor current of the DFIG with and without ADP controller.
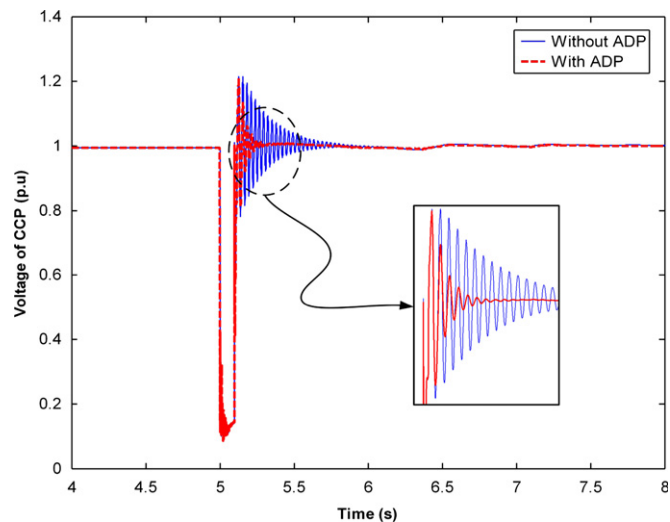

Fig. 19. Comparison of the CCP voltage with and without ADP controller at B12.
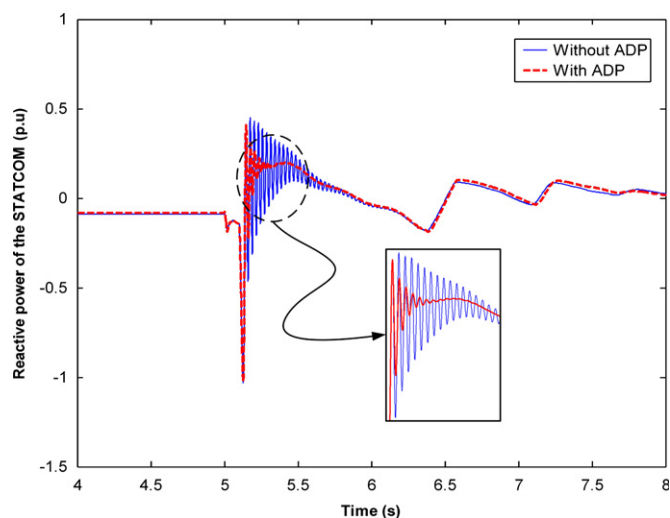

Fig. 20. Comparison of the reactive power of the STATCOM with and without ADP controller.

5. Conclusion and future work

In this paper, we investigate the reactive power control of DFIG wind turbine system based on ADP. Detailed system architecture as well as the corresponding Matlab/Simulink development have been presented in detail. Simulation results demonstrate that the ADP controller can significantly improve the dynamic performance of WT system. Specifically, our simulation results demonstrated that the sag and overshot of the active power and voltage of the wind farm can be significantly reduced after the disturbance is removed or the fault is recovered. The system stability and damping characteristic can also be improved with the ADP controller as well.

As the penetration of wind power into the power grid increases, accurate real-time control has become an important and challenging issue in the community. This requires that the control algorithm has better learning ability and better real-time interaction with the changing environment. With the recent development of new the ADP architectures, such as the hierarchically ADP design [29–32], it would be interesting to observe how such recent ADP techniques could be applied to the power system research for the smart grid development. Furthermore, in addition to modeling and simulation studies, it is critical to study the analytical characteristics of stability and robustness of the ADP approaches for power system control to provide the theoretical support of such techniques. Finally, in addition to the benchmarks as studied in this paper, it would be interesting to model and analyze relatively large and complex power system scenarios to demonstrate the applications of the ADP approaches for such a complex system control.

References

[1] U.S. Department of Energy, The smart grid: an introduction, 2008.
[2] A. Ipakchi, F. Albuyeh, Grid of the future, IEEE Power Energy Mag. (2009) 52–62.
[3] IEEE Smart Grid Initiative ⟨http://smartgrid.ieee.org/⟩.
[4] European Commission, European smart grids technology platform, 2006.
[5] A. Grauers, Efficiency of three wind energy generator system, IEEE Trans. Energy Convers. 11 (3) (1996) 650–657.
[6] R. Pena, J.C. Clear, G.M. Asher, Doubly fed induction generator using back-to-back PWM converters and its application to variable-speed wind energy generation, IEE Proc.: Electr. Power Appl. 143 (3) (1996) 231–241.
[7] V. Akhmatov, Analysis of Dynamic Behavior of Electric Power Systems with Large Amount of Wind Power, Ph.D. Dissertation, Technical University of Denmark, Kgs. Lyngby, Denmark, April 2003.
[8] F. Wu, X.P. Zhang, K. Godferey, P. Ju, Small signal stability analysis and optimal control of a wind turbine with doubly fed induction generator, IET Gener. Transm. Distrib. 1 (5) (2007) 751–760.
[9] F. Wu, X.P. Zhang, P. Ju, M.J.H. Sterling, Decentralized nonlinear control of wind turbine with doubly fed induction generator, IEEE Trans. Power Syst. 23 (2) (2008) 613–621.
[10] Y. Tang, P. Ju, H. He, C. Qin, F. Wu, Optimized control of DFIG-based wind generation using sensitivity analysis and particle swarm optimization, IEEE Trans. Smart Grid, 4 (1), (2013) 509–520, http://dx.doi.org/10.1109/TSG.2013.2237795.
[11] M. El Mokadem, V. Courtecuisse, C. Saudemont, B. Robyns, J. Deuse, Fuzzy logic supervisor-based primary frequency control experiments of a variable-speed wind generator, IEEE Trans. Power Syst. 24 (1) (2009) 407–417.
[12] H.M. Jabr, D. Lu, N.C. Kar, Design and implementation of neuro-fuzzy vector control for wind-driven doubly-fed induction generator, IEEE Trans. Sustainable Energy 2 (4) (2011) 404–413.
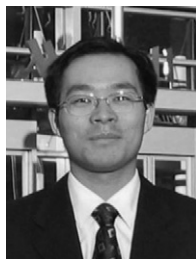
[13] L. Yang, Z. Xu, J. Ostergaard, Z.Y. Dong, K.P. Wong, Advanced control strategy of DFIG wind turbines for power system fault ride through, IEEE Trans. Power Syst. 27 (2) (2011) 713–722.

[14] A.D. Hansen, P. Sørensen, F. Iov, F. Blaabjerg, Control of variable speed wind turbines with doubly-fed induction generators, Wind Eng. 28 (4) (2004) 411–434.

[15] A. Mullane, G. Lightbody, R. Yacamini, Wind-turbine fault ride-through enhancement, IEEE Trans. Power Syst. 20 (4) (2005) 1929–1937.

[16] C. Han, A.Q. Huang, M.E. Baran, S. Bhattacharya, W. Litzenberger, L. Anderson, A.L. Johnson, A.-A. Edris, STATCOM impact study on the integration of a large wind farm into a weak loop power system, IEEE Trans. Energy Convers. 23 (1) (2008) 226–233.

[17] P.J. Werbos, Computational intelligence for the smart grid-history, challenges, and opportunities, IEEE Comput. Intell. Mag. 6 (3) (2011) 14–21.

[18] G.K. Venayagamoorthy, Dynamic, stochastic, computational, and scalable technologies for smart grids, IEEE Comput. Intell. Mag. 6 (3) (2011) 22–35.

[19] W. Qiao, R.G. Harley, G.K. Venayagamoorthy, Coordinated reactive power control of a large wind farm and a STATCOM using heuristic dynamic programming, IEEE Trans. Energy Convers. 24 (2) (2009) 493–503.

[20] W. Qiao, G.K. Venayagamoorthy, R.G. Harley, Real-time implementation of a STATCOM on a wind farm equipped with doubly fed induction generators, IEEE Trans. Ind. Appl. 45 (1) (2009) 98–107.

[21] J. Fu, H. He, X. Zhou, Adaptive learning and control for mimo system based on adaptive dynamic programming, IEEE Trans. Neural Networks 22 (7) (2011) 1133–1148.

[22] J. Si, Y.T. Wang, Online learning control by association and reinforcement, IEEE Trans. Neural Networks 12 (2) (2001) 264–276.

[23] R. Enns, J. Si, Apache helicopter stabilization using neuro-dynamic programming, J. Guid. Control Dyn. 25 (1) (2002) 19–25.

[24] R. Enns, J. Si, Helicopter trimming and tracking control using direct neural dynamic programming, IEEE Trans. Neural Networks 14 (4) (2003) 929–939.

[25] C. Lu, J. Si, X. Xie, Direct heuristic dynamic programming for damping oscillations in a large power system, IEEE Trans. Syst. Man Cybern. Part B: Cybern. 38 (4) (2008) 1008–1013.

[26] X. Fang, H. He, Z. Ni, Y. Tang, Learning and control in virtual reality for machine intelligence, in: 2012 Third International Conference on Intelligent Control and Information Processing (ICICIP), July 2012, pp. 63–67.

[27] Y. Tang, H. He, J. Wen, Adaptive control for an HVDC transmission link with FACTs and a wind farm, in: Proceedings of the IEEE Innovative Smart Grid Technologies Conference (ISGT'13), Washington, February, 2013.

[28] Y. Tang, H. He, J. Wen, Comparative study between HDP and PSS on DFIG damping control, in: IEEE Symposium Series on Computational Intelligence, May 2013.

[29] H. He, Self-Adaptive Systems for Machine Intelligence, Wiley, 2011, ISBN: 978-0-470-34396-8.

[30] H. He, Z. Ni, J. Fu, A three-network architecture for on-line learning and optimization based on adaptive dynamic programming, Neurocomputing 78 (1) (2012) 3–13.

[31] Z. Ni, H. He, J. Wen, Adaptive learning in tracking control based on the dual critic network design, IEEE Trans. Neural Networks Learn. Syst., PP (99), 1,1, 0 http://dx.doi.org/10.1109/TNNLS.2013.2247627.

[32] H. He, Z. Ni, D. Zhao, Learning and optimization in hierarchical adaptive critic design, in: Reinforcement Learning and Approximate Dynamic Programming for Feedback Control, Wiley-IEEE Press, 2013, pp. 78–95.

intelligence, self-adaptive systems, machine learning, data mining, embedded intelligent system design (VLSI/FPGA), and various applications such as smart grid, cognitive radio, sensor networks, and others. He has published 1 sole-author research book with Wiley, edited 6 conference proceedings with Springer, and authored and co-authored over 100 peer-reviewed journal and conference papers. His research results have been covered by national and international medias such as The Wall Street Journal, Yahoo!, Providence Business News, among others. He has delivered numerous invited talks. He is currently a member of various IEEE Technical Committees, and also served as various conference chairship positions for numerous international conferences. He has been a Guest Editor for several journals including IEEE Computational Intelligence Magazine, Cognitive Computation (Springer), Applied Mathematics and Computation (Elsevier), Soft Computing (Springer), among others. Currently, he is an Associate Editor of the IEEE Transactions on Neural Networks and Learning Systems, and IEEE Transactions on Smart Grid, and also serves on the Editorial Board for several international journals. He received the National Science Foundation (NSF) CAREER Award (2011) and Providence Business News (PBN) "Rising Star Innovator" Award (2011). He is a Senior Member of IEEE.
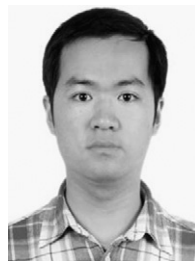
Zhen Ni received his B.S. degree in the Department of Control Science and Engineering from Huazhong University of Science and Technology, China, in 2010. He is currently a Ph.D. student in the Department of Electrical, Computer, and Biomedical Engineering, University of Rhode Island, RI, USA. His major research interests include adaptive dynamic programming, reinforcement learning, and computational intelligence.

Jinyu Wen is the vice dean of the College of Electrical and Electronic Engineering at Huazhong University of Science and Technology in Wuhan, China. He leads the Smart Grid Operation & Control Research Group in the China State Key Laboratory of Advanced Electromagnetic Engineering and Technology. His research interests include smart grid, power system operation and control, renewable energy systems, and energy storage. He is an active member of the IEEE Power & Energy Society and Industry Application Society.

Xianchao Sui received the B.S. and M.S. degrees in electrical engineering from Huazhong University of Science and Technology (HUST), Wuhan, China, in 2008 and 2011, respectively. His research interests include smart grid, renewable energy, and power system control. He is currently working in State Grid, Dalian, China.

Yufei Tang received the B.Eng. and M.Eng. degrees in electrical engineering from Hohai University, Nanjing, China, in 2008 and 2011, respectively, and is currently pursuing the Ph.D. degree in the Department of Electrical, Computer, and Biomedical Engineering, University of Rhode Island, Kingston.

His research is focused on power system modeling, dynamics, control and stability, wind energy generation and integration, and the application of computational intelligence in power systems.

Haibo He received the B.S. and M.S. degrees in electrical engineering from Huazhong University of Science and Technology, China, in 1999 and 2002, respectively, and the Ph.D. degree in electrical engineering from Ohio University in 2006. He is currently an Associate Professor at the Department of Electrical, Computer, and Biomedical Engineering, University of Rhode Island. From 2006 to 2009, he was an Assistant Professor at the Department of Electrical and Computer Engineering, Stevens Institute of Technology.

His current research interests include computational